SCIENCE CHINA
Physics, Mechanics & Astronomy

• Article •

January 2014 Vol.57 No.1: 166–175
doi: 10.1007/s11433-013-5181-7

GNSS clock corrections densification at SHAO: from 5 min to 30 s

CHEN JunPing[1*], ZHANG YiZe[1,2], ZHOU XuHua[1], PEI Xiao[1,2], WANG JieXian[2] & WU Bin[1]

[1] *Shanghai Astronomical Observatory, Chinese Academy of Sciences, Shanghai 200030, China;*
[2] *College of Surveying and Geo-Informatics, Tongji University, Shanghai 200092, China*

Received January 7, 2013; accepted March 26, 2013; published online July 10, 2013

High frequency multi-GNSS zero-difference applications like Precise Orbit Determination (POD) for Low Earth Orbiters (LEO) and high frequency kinematic positioning require corresponding high-rate GNSS clock corrections. The determination of the GNSS clocks in the orbit determination process is time consuming, especially in the combined GPS/GLONASS processing. At present, a large number of IGS Analysis Centers (AC) provide clock corrections in 5-min sampling and only a few ACs provide clocks in 30-s sampling for both GPS and GLONASS. In this paper, an efficient epoch-difference GNSS clock determination algorithm is adopted based on the algorithm used by the Center for Orbit Determination in Europe (CODE). The clock determination procedure of the GNSS Analysis Center at Shanghai Astronomical Observatory (SHAO) and the algorithm is described in detail. It is shown that the approach greatly speeds up the processing, and the densified 30-s clocks have the same quality as the 5-min clocks estimated based on a zero-difference solution. Comparing the densified 30-s GNSS clocks provided by SHAO with that of IGS and its ACs, results show that our 30-s GNSS clocks are of the same quality as that of IGS. Allan deviation also gives the same conclusion. Further validation of the SHAO 30-s clock product is performed in kinematic PPP and LEO POD. Results indicate that the positions have the same accuracy when using SHAO 30-s GNSS clocks or IGS (and its AC) finals. The robustness of the algorithm and processing approach ensure its extension to provide clocks in 5-s or even higher frequencies. The implementation of the new approach is simple and it could be delivered as a black-box to the current scientific software packages.

satellite clock corrections, GNSS, epoch-difference, clock densification, kinematic precise point positioning

PACS number(s): 91.10.Fc, 95.10.Eg, 93.85.Bc, 93.30.Db

Citation: Chen J P, Zhang Y Z, Zhou X H, et al. GNSS clock corrections densification at SHAO: from 5 min to 30 s. Sci China-Phys Mech Astron, 2014, 57: 166–175, doi: 10.1007/s11433-013-5181-7

1 Introduction

Precise Point Positioning (PPP) [1] has been widely discussed over the past ten years in Precise Orbit Determination (POD) for Low Earth Orbiters (LEO) [2–4] and kinematic positioning [5]. Unlike differential positioning, PPP use non-differenced phase and pseudo-range observations and the accuracy of PPP applications depends on the accuracy of GNSS orbits and clocks. Currently, the International GNSS Service [6] has provided a precise GNSS satellite orbits product at the interval of 15 min. It can be interpolated with almost no degradation of accuracy at the user-needed epoch by sliding polynomial interpolation [7]. However, the accuracy of satellite clocks dramatically degrade with the increase of interpolation interval and no proper method can solve this problem well. Conventional satellite clock estimation istime consuming work with the

*Corresponding author (email: junping.chen@shao.ac.cn)

increase of data sampling and size of network because a zero-difference solution has to be used in clock estimation. Because of this, many IGS analysis centers provide satellite clocks only in 5-min intervals or they use only a sub-network to provide precise clocks.

With the development of the GLONASS system, multi-GNSS applications including PPP emerge as a big enhancement to the current applications. GLONASS uses a frequency division multiple access (FDMA) technique to distinguish signals from different satellites [8]. In combined GPS/GLONASS analysis, we should consider the inter-system bias (ISB) between the two systems and the inter-frequency bias (IFB) between GLONASS satellites. As a result, the parameters to be estimated are increased by a large amount, which introduces further challenges for the production of high-rate GNSS clocks. Since GPS week 1686, GLONASS satellite clocks are available in three analysis centers, namely ESA, GFZ and IAC. Among these three ACs, only ESA provides 30-s GLONASS satellite clocks.

To improve the availability of precise GNSS products and to shorten the time of products releasing, we set up the GNSS Analysis Center at Shanghai Astronomical Observatory (SHAO) [9]. The analysis center (abbreviated as SHA) follows the IGS AC strategies and aims to fulfill the requests of satellite missions in China. By the end of 2011, SHA started the provision of 30-s GNSS clocks—which means that we not only provide 30-s GPS clocks, but also that of GLONASS. SHA 30-s GNSS clocks are generated by two steps: firstly, precise GNSS orbits, earth rotation parameters (ERPs), station coordinates, tropospheric parameters and GNSS clocks are estimated using a zero-difference approach based on 5-min sampling data of selected global GNSS network; secondly, the GNSS orbits, tropospheric parameters and station coordinates are introduced and kept fixed in an epoch-differenced solution, where cleaned data with 30-s sampling is used and only GNSS clocks are estimated.

Sect. 2 describes the epoch-differenced algorithm for the GNSS satellite clocks densification, and a simple but effective method to regularize normal equations is introduced. In sect. 3, the routine combined GNSS data processing procedure at SHAO is introduced. In sect. 4, the quality of the high-rate GNSS clocks provided by SHAO are assessed. Sect. 5 applies the SHA densified GNSS clocks in kinematic PPP and POD to validate their quality. Sect. 6 gives the conclusion. The implementation of the epoch- difference approach developed in this paper is easy, which could be delivered as a black-box to the current software packages like BERNESE, EPOS, GAMIT, or GIPSY. Due to its robustness and reliability, the algorithm and processing scheme could be precisely extended to provide clocks in 5-s or even higher frequencies.

2 GNSS clock densification algorithm

To obtain precise and continuous GNSS orbits and clocks, a globally distributed network with 50–250 stations is processed by the IGS ACs. Generally, there are two strategies within the IGS for the generation of clock products, namely the non-differential and differential strategies. In the non-differential strategy, satellite clocks are estimated together with other parameters in a zero-difference solution. The differential strategy includes two steps: firstly, parameters like GNSS orbits, station coordinates, tropospheric parameters and ERPs are estimated by forming a double-difference solution; these parameters are fixed in the second step and a zero-difference solution is performed to obtain the clocks corrections. Both the non-differential and differential approaches have to use the zero-difference solution for clock estimation.

In the zero-difference solution, the number of parameters to be estimated increases dramatically with the number of satellites and stations. Taking the combined GPS/ GLONASS solution including 32 GPS satellites and 24 GLONASS satellites as an example, Figure 1 shows the number of estimated parameters increasing with the number of stations in the network for the case of a GPS-only and a combined GPS/GLONASS solution. As the clock parameters are usually eliminated epoch-by-epoch [10], only those clocks at one single epoch are accounted. Figure 1 assumes two ambiguities per station/satellite pair, 15 orbit parameters per satellite and 12 ZTD parameters for each station. As for the network with 100 stations, there are about 6400 ambiguity parameters, 100 receiver clocks, 32 satellite clocks, 300 station coordinates, 470 orbit parameters, 1200 ZTD parameters and 6 ERP parameters for a daily GPS-only solution. In the case of a combined daily GPS/GLONASS solution, there are additionally 1200 (number of GLONASS frequency x number of stations) ISB and 4800 GLONASS ambiguity parameters. Considering the huge number of parameters, a traditional least square estimator would generally fail to solve the normal equation (NEQ). This problem becomes even worse if the number of stations increases. As shown in Figure 1, the number of ambiguities increases remarkably faster than that of the other parameters. In the case of a combined daily GPS/GLONASS solution using 200 stations, the total number of unknown parameters exceeds 30000.

There are strategies trying to solve this problem [10]. The main idea is parameter elimination: firstly epoch-wise parameters (clocks) are eliminated from the NEQ epoch-by-epoch and piece-wise-constant parameters (ambiguities and ZTDs) are eliminated piece by piece; after solving for the daily constant parameters, those eliminated parameters are recovered by substitution. Parameter elimination involves inversion of the NEQ, and the computation problem still exists if the number of to-be eliminated parameters is huge.

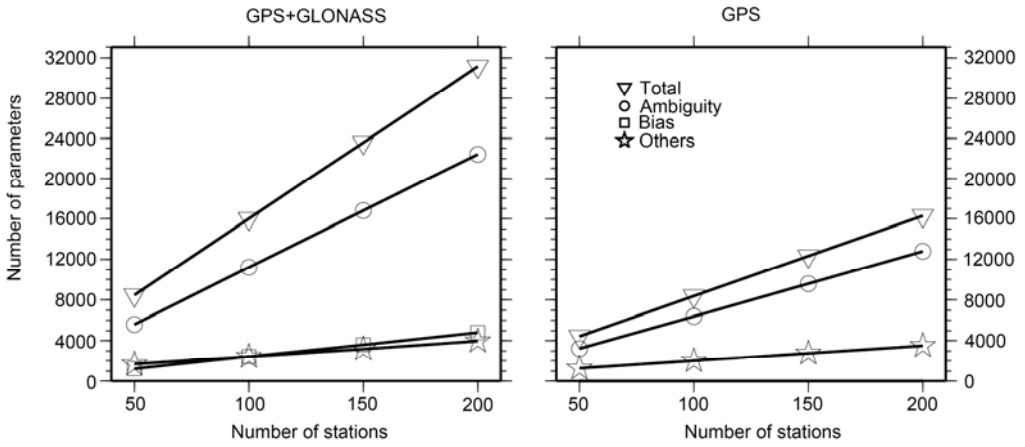

Figure 1 Growth of the number of ambiguities and other parameters versus the increase of the number of stations tracking a constellation of 32 GPS satellites and 24 GLONASS satellites.

Taking the GPS-only solution as an example, the computation time is around 2 min for one iteration using the network of 100 stations with 5-min sampling. However, it takes around 43 min for one iteration if the number of stations is increased to 250. In the case of GPS/GLONASS combined analysis, according to our experiences the computation time is about 4 times more than a GPS-only solution. Considering the many iterations performed normally in precise data analysis, the computation time is even more than 12 h for a daily GPS/GLONASS combined solution.

To solve the problem, we have to reduce the number of parameters. Two approaches are currently used within IGS: the first one is using a double-difference to remove clock parameters and reduce the number of ambiguities; the second one is using a zero-difference with longer time interval (e.g., 5 min) to reduce the number of clock parameters. The double-difference procedure has been used in many IGS ACs, e.g., MIT, CODE, etc. Using this approach, they have to reproduce clocks using the zero-difference approach with a sub-network. The zero-difference procedure is used by GFZ, JPL etc., and they can generate only 5-min clocks.

Following this discussion, the generation of 30-s clocks together with other parameters is time consuming. Bock developed an efficient method to densify the GPS clock corrections from 5 min to 30 s and 5 s [11]. The general concept contains three steps: estimation of low-rate (e.g., 5 min) clocks in the orbit determination process; estimation of a high-rate epoch-differenced clock; and combining epoch-differenced clocks and the low-rate clocks. In their algorithm, they combine the equations of all epochs into one NEQ, which needs a special algorithm for the solution. In the following, we adopt their algorithm to allow a piecewise (in 5 min) solution and extend it to the GPS/GLONASS combined clock densification.

2.1 Epoch-differenced GNSS clocks estimation

For station k, ionosphere-free GNSS LC combination at epoch t_i reads as:

$$\begin{cases} L_k^G(t_i) = \rho_k^G(t_i) + c\cdot\delta_k(t_i) - c\cdot\delta^G(t_i) \\ \qquad + \delta_{\mathrm{Trop}}^G(t_i) + \lambda_G\cdot N_k^G + \varepsilon_k^G(t_i), \\ L_k^R(t_i) = \rho_k^R(t_i) + c\cdot\delta_k(t_i) + c\cdot\delta_{k,\mathrm{ISB}} \\ \qquad - c\cdot\delta^R(t_i) + \delta_{\mathrm{Trop}}^R(t_i) + \lambda_R\cdot N_k^R + \varepsilon_k^R(t_i), \end{cases} \tag{1}$$

where G, R stand for GPS and GLONASS, L_k is the ionosphere-free phase observation, ρ_k is the geometric range between satellite and receiver, δ_k is the receiver clock correction, δ^G and δ^R are the GPS and GLONASS satellite clock corrections, $\delta_{k,\mathrm{ISB}}$ is the ISB between GPS and GLONASS, δ_{Trop} is the tropospheric delay, N_k is the ambiguity, λ is the ionosphere-free combination wavelength, ε_k is the noise of combined phase observation, and c is the speed of light.

If there are no cycle slips between two adjacent epochs i+1 and i, and considering the ISB as a daily constant for each station/frequency pair, the ambiguity term and ISB term $\delta_{k,\mathrm{TO}}$ can be eliminated by forming an epoch-differenced equation.

$$\begin{cases} \Delta L_k^G(t_{i+1,i}) = \Delta\rho_k^G(t_{i+1,i}) + c\cdot\Delta\delta_k(t_{i+1,i}) - c\cdot\Delta\delta^G(t_{i+1,i}) \\ \qquad + \Delta\delta_{\mathrm{Trop}}^G(t_{i+1,i}) + \Delta\varepsilon_k^G(t_{i+1,i}), \\ \Delta L_k^R(t_{i+1,i}) = \Delta\rho_k^R(t_{i+1,i}) + c\cdot\Delta\delta_k(t_{i+1,i}) - c\cdot\Delta\delta^R(t_{i+1,i}) \\ \qquad + \Delta\delta_{\mathrm{Trop}}^R(t_{i+1,i}) + \Delta\varepsilon_k^R(t_{i+1,i}), \end{cases} \tag{2}$$

where "Δ" indicates the difference operator.

In eq. (2), station coordinates, tropospheric parameters, and GNSS orbits are precisely estimated in the previous orbit determination step. Therefore, the geometric term and tropospheric term can be removed and eq. (2) can be rewritten as:

$$\begin{cases} \Delta L_k^G(t_{i+1,i}) = c\cdot\Delta\delta_k(t_{i+1,i}) - c\cdot\Delta\delta^G(t_{i+1,i}) + \Delta\varepsilon_k^G(t_{i+1,i}), \\ \Delta L_k^R(t_{i+1,i}) = c\cdot\Delta\delta_k(t_{i+1,i}) - c\cdot\Delta\delta^R(t_{i+1,i}) + \Delta\varepsilon_k^R(t_{i+1,i}). \end{cases} \tag{3}$$

In eq. (3), only the epoch-differenced GNSS satellite clocks and station clocks are estimated, which greatly reduces the size of the NEQ and decreases the computation time. Eq. (3) applies also to the estimation of GLONASS epoch-differenced clocks as the ISB term is removed by forming the epoch difference.

In eq. (3), the NEQ is rank defect. Similar to the general procedure in the orbit determination, a reference clock could be introduced as datum into the epoch-wise NEQ to overcome this problem. Following the conventional procedure of IGS data analysis, the 5-min GNSS clocks generated at SHA have been aligned to the GPS broadcast, by which the clock datum is stable and the clock interpolation error from 5 min to 30 s can be ignored for the reference maser clock. Considering this, epoch-differenced clocks of the reference clock are regarded as pseudo-observations and are heavily constrained. In our analysis, their weight are normally larger than 1000. Applying this method, a list of reference stations is prepared in a table. In cases of discontinuity in the reference station data, we could switch to another reference clock from that epoch.

The epoch-difference measurements between subsequent observation epochs are correlated as long as they are connected by at least one ambiguity term, as it was pointed out by Bock et al. [11] that the simplifications not considering these correlations are allowed over short time intervals of 5 min without losing precision for the clock estimates.

Meanwhile, we get the variance of the epoch-differenced clocks $\sigma(t_{i+1,i})$ for stations, $\sigma^G(t_{i+1,i})$ for GPS satellites and $\sigma^R(t_{i+1,i})$ for GLONASS satellites. They are used in the following procedure of GNSS clocks densification.

2.2 GNSS clock densification

By using the epoch-differenced phase combination, the epoch-differenced GNSS clocks $\Delta\delta(t_{i+1,i})$ are epoch-wisely estimated at a sampling of 30 s. To derive the absolute clocks, one solution is to define absolute clocks at a reference epoch and the epoch-differenced clocks are summed up in other epochs. Absolute clocks from this approach depend on the values of the reference epoch and thus may differ from the input 5-min clocks at a common sampling epoch. Also the sum will amplify noise and introduce additional errors. A better approach is to combine epoch-differenced (sampling 30 s) and zero-differenced clocks (sampling 5 min).

For a particular clock, such combinations could be written as:

$$\begin{cases} -\delta(t_1)+\delta(t_2) = \Delta\delta(t_{2,1}), \\ -\delta(t_2)+\delta(t_3) = \Delta\delta(t_{2,1}), \\ \cdots \\ -\delta(t_{11})+\delta(t_{10}) = \Delta\delta(t_{11,10}), \end{cases} \tag{4}$$

with constraints

$$\begin{cases} \delta(t_1) = \delta_{\text{fix}}(t_1), \\ \delta(t_{11}) = \delta_{\text{fix}}(t_{11}). \end{cases} \tag{5}$$

In eq. (4), δ_1, δ_2, δ_3, …, δ_{11} are the 30-s clocks of the time-period of 5 min, where the clocks at the first and last epoch, i.e., δ_1 and δ_{11}, are determined precisely as $\delta_{\text{fix}}(t_1)$ and $\delta_{\text{fix}}(t_{11})$ in the previous orbit determination step.

Neglecting the correlations between two epoch-differenced solutions, the weights in eq. (4) can be defined as:

$$p(t_{i+1,i}) = \frac{\sigma_0^2}{\sigma^2(t_{i+1,i})}, \tag{6}$$

where $\sigma(t_{i+1,i})$ is derived in the epoch-differenced clocks estimation. Due to the special structure of eqs. (4) and (5), the parameter in eq. (4) can be expressed as:

$$\delta(t_{i+1}) = \delta\left(t_i\right) + \Delta\delta\left(t_{i+1,i}\right) + \frac{1}{p\left(t_{i+1,i}\right)}\mathrm{d}\delta,\ i = 1, 2, \cdots, 10, \tag{7}$$

where

$$\mathrm{d}\delta = \left(\delta(t_{11}) - \delta(t_1) - \sum_{j=1}^{10}\Delta\delta\left(t_{j+1,j}\right)\right) \Bigg/ \sum_{j=1}^{10}\frac{1}{p\left(t_{j+1,j}\right)}\sqrt{2}.$$

Using this algorithm, the densification of GNSS clocks is performed at each 5-min piece satellite-by-satellite and station-by-station.

The epoch-difference clocks and the absolute clocks generated based our approach rely on reference clocks, and eventually on the GPS time scale (as our clocks are aligned to the GPS broadcast). Due to the high stability of the reference time scale, the same algorithm and processing scheme could be used for clock generation of 5-s or even higher frequencies.

3 Clock correction determination procedures at SHA

The clock densification algorithm has been integrated into the GNSS routine analysis at the GNSS analysis center of SHAO. The analysis center was established to improve the availability of precise GNSS products for users in China, and to shorten the time of products releasing, thus meeting the requirement of some special applications where precise orbits and clocks are required with latency less than 2 h. Currently, our GNSS routine analysis includes global GPS+GLONASS data processing and global + CMONOC GPS data processing. In the first routine, we use ~110 global stations, shown in Figure 2, of which ~50 have GLONASS observations, to derive the integrated and consistent GNSS products. In the second routine, we combine the IGS net-

work used in the first routine and the CMONOC (Crustal Movement Observation Network of China) network, shown in Figure 3, and a GPS-only solution is performed using ~300 stations.

The GNSS clocks determination procedure is part of our GNSS routine jobs using the GNSS analysis package developed at SHAO. The parameter estimation procedures within the GNSS package are based on a classical least squares adjustment. The underlying physical models for the data processing are based on the IERS conventions [12]. A GNSS orbit determination procedure based on a zero-difference technique is the core of the SHA analyses. In the zero-difference approach, most of the parameters, including GNSS orbit parameters, ERPs, coordinates, tropospheric parameters, clocks, etc, are estimated. The raw GNSS observations are cleaned with sampling of 30 s. As previously discussed, zero-difference data processing using a network with ~300 stations is time consuming and therefore the sampling rate of observations is set to 5 min in the parameter estimation step. Satellite clocks of 5-min sampling are derived for both GPS and GLONASS and GPS/GLONASS ISB parameters are estimated as a daily constant for each station/frequency pair. In this step, a reference clock is selected from a pre-defined list which contains most stable clocks in the IGS network. A sophisticated procedure is set up for the selection of the reference clock, which ensures that there is no data gap for the reference clock and the reference clock is ultimate stable in a linear-trend. Compari-

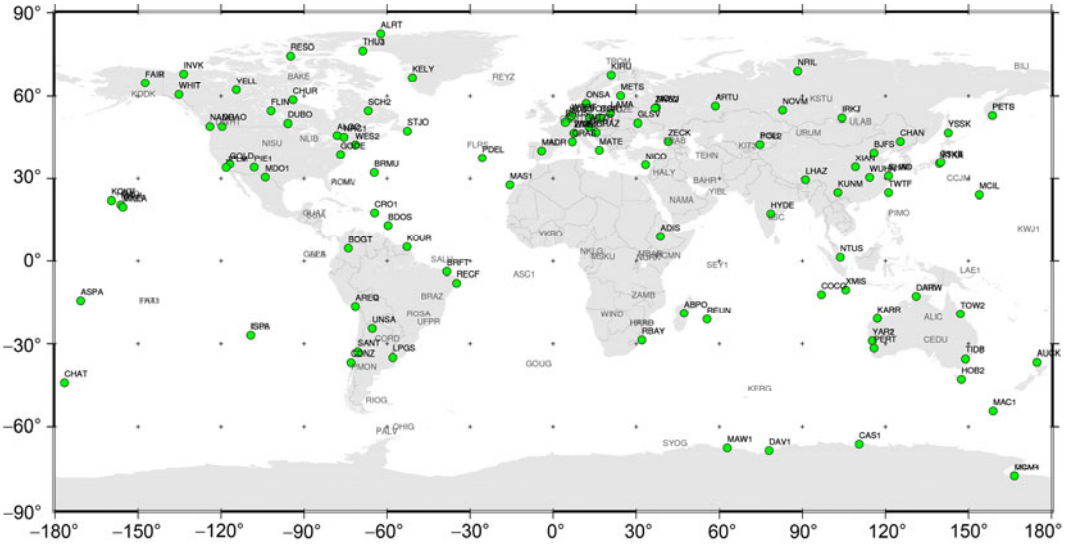

Figure 2 (Color online) IGS network processed in the GNSS routine of SHA.

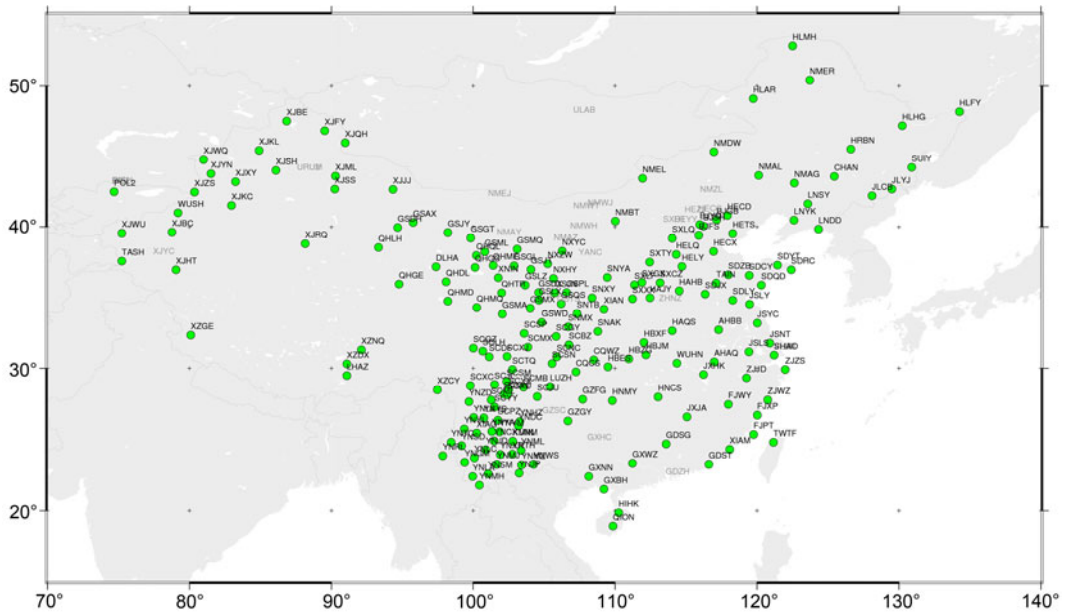

Figure 3 (Color online) CMONOC network processed in the GNSS routine of SHA.

sons between our combined GPS/GLONASS orbits and the IGS finals using 18 months of products show that the precision (RMS) is of 1.8 cm for our GPS orbits and 3.8 cm for GLONASS orbits.

After the orbit determination step, the GNSS clock densification procedure based on the above-described algorithm is performed. For this clock densification the GNSS orbits, ERPs, station coordinates, and tropospheric parameters are taken from the orbit determination step. The same list of stations and the cleaned observations sampling at 30 s are used. Figure 4 summarizes the GNSS clock estimation procedure at SHAO. The average computation time of the clock densification procedure is about 3 min (in a Linux environment with 2.40 GHz CPU processors), which indicates the efficiency of this approach.

In step two, to ensure the quality of the densified GNSS clocks at the beginning and end of a day, an additional the few epochs of GNSS orbit is needed for precise orbit interpolation, which could be easily obtained by extending the orbit integration period in the first step. To avoid the impact of reference clock jumps, a list of reference clocks could be used. When a clock jump happens between two adjacent epochs at the reference station, another reference clock is used. As for the SHA analysis center, these selected reference clocks are always hydrogen maser clocks, including AMC2 (Colorado Springs, USA), WTZR (Bad Koetzting, Germany), WSRT (Westerbork, Netherlands), PIE1 (Pie Town, USA), ONSA (Onsala, Sweden), KOKB (Kokee Park, USA), USN3 (Washington, USA), NRC1 (Ottawa, Canada), NLIB (North Liberty, USA), TID2 (Tidbinbilla, Australia) and NISU (Boulder, USA).

4 Quality of the SHA GNSS clocks

4.1 Clock comparison with IGS clocks

To assess the quality of the densified 30-s GNSS clocks, we calculate the differences between our clocks and the IGS final clocks. Following the standard process in the IGS clock comparison, the resulting time series are aligned to a reference satellite in order to remove possible systematic biases [13,14]. The bias and standard deviation (STD) of each satellite are computed. Furthermore, we use the RMS of the clock differences as quality indicators to measure the satellite-specific bias. A larger RMS indicates more inconsistency of the clocks, which directly propagate into range modeling and will be absorbed by the ambiguity parameters in phase data.

Tables 1 and 2 summarize the two above-mentioned mean quality indices of our clocks (5-min and 30-s sampling) compared to the final clocks of IGS, IGR, COD, EMR, ESA, GFZ, GRG, IAC and JPL over a period of 4 weeks (GPS week 1686–1689). For the comparison, the GPS clocks of IGR, GFZ and JPL are sampled at 5 min and the others (except IAC) are of 30-s sampling. The GLONASS clocks sampling is of 30 s for ESA and 5 min for GFZ. The GLONASS clocks of other ACs (EMR, GRG and IAC) are retrieved from their SP3 files sampled at 15 min. From quality indices in the two tables, the results of the densified 30-s sampling and 5-min sampling original clocks show little difference. GPS clocks of SHA are closest to the IGS Rapid clocks with a STD of 41 ps and RMS of 82 ps. GLONASS clocks of SHA are closest to the GFZ final

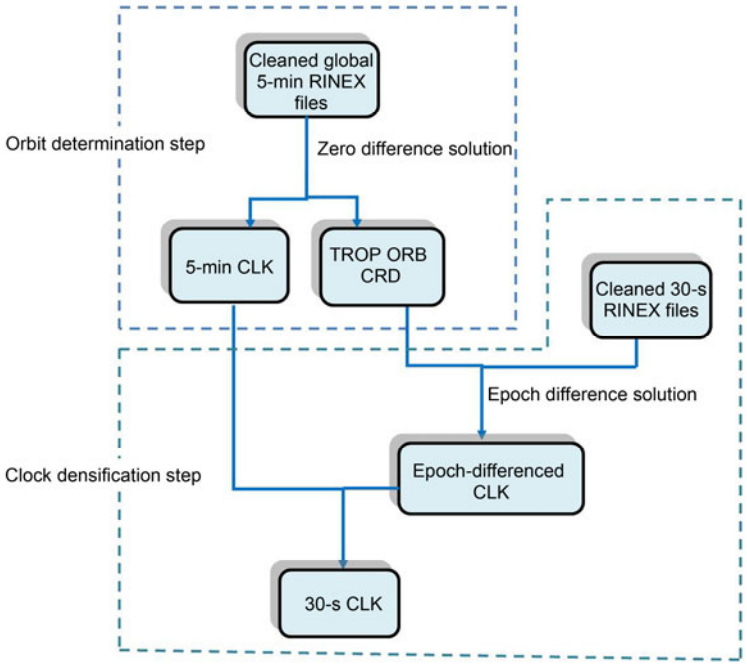

Figure 4 (Color online) Flow Chart of the 30-s GNSS clock generation (CLK: clocks, TROP: tropospheric parameters, ORB: GNSS orbits, CRD: coordinates).

Table 1 STD of clocks at SHA compared with other ACs (in ps), '–' means no product available

Sampling	COD	EMR	ESA	GFZ	GRG	IAC	IGS	IGR	JPL
				GPS					
5-min	63	86	50	43	70	–	43	41	85
30-s	64	96	52	44	70	–	44	41	87
				GLONASS					
5-min	–	102	104	83	130	140	–	–	–
30-s	–	113	110	85	132	141	–	–	–

Table 2 RMS of clocks at SHA compared with other ACs (in ps), '–' means no product available

Sampling	COD	EMR	ESA	GFZ	GRG	IAC	IGS	IGR	JPL
				GPS					
5-min	113	142	102	85	148	–	87	82	140
30-s	113	143	103	85	157	–	88	82	143
				GLONASS					
5-min	–	407	3345	348	11670	1561	–	–	–
30-s	–	408	3356	353	11701	1565	–	–	–

clocks with a STD of 85 ps and RMS of 353 ps. GLONASS clocks are generally worse than GPS clocks because the distribution of stations tracking GLONASS satellites is poorer. The large RMSs in GLONASS clock comparisons indicate different GLONASS inter-frequency biases of each AC, which is related to the different strategies in IFB handling. The comparison indicates our IFB modeling is similar to that of GFZ and EMR, while the strategy of ESA, GRG, and IAC are different. Of the four weeks' comparisons, daily RMS varies a lot for the comparisons with GRG, while it is quite smooth for the comparisons with the others.

4.2 Allan deviation study

Allan deviation is a measure of frequency instability in clocks or oscillators [15,16]. A similar Allan deviation spectrum indicates similar clock quality. In this part we use Allan deviation to assess the quality of densified 30-s clocks.

Taking the day 120 of the year 2012 for example, the receiver clock of AMC2, steered by a hydrogen maser clock, is used as a reference clock and 5-min clocks are estimated firstly in the zero-difference orbit determination step. Applying the above-developed clock densification method, 30-s clocks are generated for both GPS/GLONASS satellites and stations. Figure 5 shows the Allan deviation of three stations: DAV1 steered by a Rubidium clock, SYOG steered by a Cesium clock and WTZR steered by a Hydrogen clock. Figure 6 shows the Allan deviation for five satellite clocks, representing satellite groups of GPS Block IIA (Cesium), Block IIR (Rubidium), Block IIR-M (Rubidium), Block IIF (Rubidium) and GLONASS-M (Cesium), respectively. In these figures, SHA clocks of 5 min and 30 s and IGS final clocks of 30-s sampling (5-min for stations) are plotted with time interval from 5 to 30000 s. From the two figures we see that Allan deviation of SHA clocks at different sampling intervals are the same, which proves that the densified 30-s clocks have the same quality of the original 5-min clocks. In general, the spectra of SHA clocks are similar to those of IGS clocks, which further confirms that SHA clocks have the same quality as IGS clocks. IGS clocks are more stable for some clocks, e.g., WTZR and G25, which is due to the fact that IGS final clocks are aligned to a more stable time scale (IGST), a weighted ensemble of a number of tracking receivers using external hydrogen-maser [17].

5 Application of 30-s GNSS clocks

5.1 Validation in kinematic PPP

High-rate kinematic PPP requires precise high-rate GNSS satellite clocks. Using the same software as for orbits and clocks production to perform PPP results in the best accuracy, as there is better system consistency. To reduce the inner-consistency and to reflect the system biases, Bernese software [18] is used for kinematic PPP. GPS/GLONASS data of the stable IGS station SHAO (Shanghai, China) covering days 120–126 of the year 2012 have been processed. We set up 3 scenarios: a GPS-only solution, a GLONASS-solution and a GPS/GLONASS combined solution. For all 3 scenarios, we use SHA GNSS clocks of 30-s and 5-min sampling and ESA GNSS clocks of 30-s sampling. Corresponding orbits are used together with clocks. For validation, all kinematic coordinates are compared to the IGS "ground true". The comparison shows the biggest differences in the upper component, which is due to two facts: the upper component normally has more noise than the horizontals; and clock differences mainly affect the upper component.

Table 3 summarizes the comparisons, showing the mean RMS in the upper component and in 3-D. From Table 3 we see that the two result sets based on 30-s clocks are quite similar, which suggests that our 30-s clocks have the same precision as other IGS ACs. And the solutions based on

5-min are degraded by a factor of up to 1.8. We conclude also from Table 3 that interestingly GLONASS stand-alone solutions are better than GPS-only solutions for this station. Combined GPS/GLONASS kinematic PPP has the best results and is close to the GLONASS-only solution with a 3-D RMS of 1.9 cm, which has an improvement of up to 34% over GPS-only kinematic PPP.

5.2 Validation in LEO POD for gravity field determination

One of the important applications of high-rate satellite clocks is POD for low earth orbit. Kinematic positions of LEO referring to different epochs contain gravity field information and are independent at each epoch. The kinematic positions are thus helpful to significantly reduce the propagation of the positioning errors into the estimated gravity field coefficients [19]. GPS tracking data of GRACE-A and GRACE-B covering days 94–100 of the year 2010 have been used to show the benefit of high-rate GNSS clocks in kinematic POD. GRACE GPS data with 10-s sampling is used and kinematic solutions have been computed using an in-house developed LEO POD software package [20].

As the influence of clock errors is mainly reflected in the

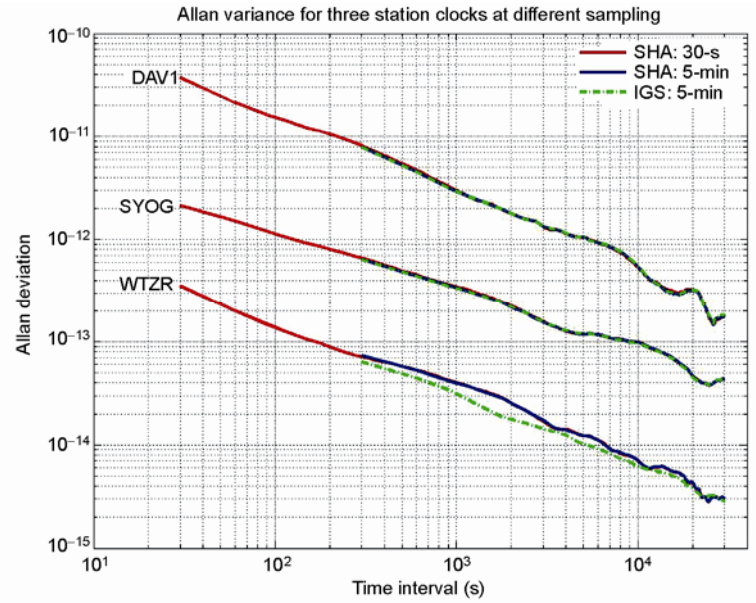

Figure 5 Allan deviation of SHA clocks of 30-s and 5-min sampling and IGS final clocks of 5-min sampling for station stations DAV1, SYOG and WTZR, day 120, 2012.

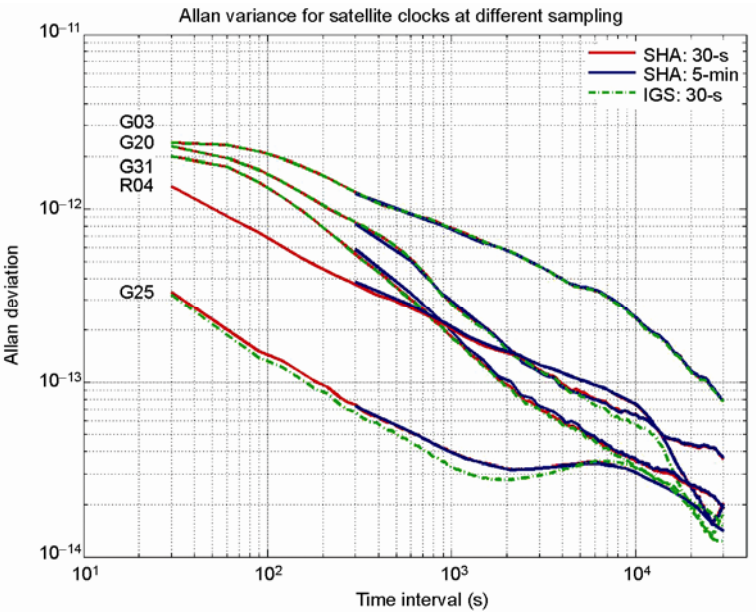

Figure 6 Allan deviation of SHA clocks of 30-s and 5-min sampling and IGS final clocks of 30-s sampling for five kinds of satellites (G03 for Block IIA, G20 for Block IIR, G31 for Block IIR-M, G25 for Block IIF, R04 for GLONASS-M), day 120, 2012. Allan deviation of R04 is not plotted because there are no official IGS GLONASS clocks.

Table 3 Mean RMS (cm) in the upper component and in 3-D for kinematic GPS/GLONASS PPP using clocks from ESA final (30-s sampling) and SHA (5-min and 30-s sampling), days 120–126, 2012

	GPS		GLONASS		GPS/GLONASS	
	Up	3-D	Up	3-D	Up	3-D
SHA: 5-min	3.2	4.0	2.3	3.2	2.5	3.5
SHA: 30-s	2.1	2.9	1.5	1.9	1.4	1.9
ESA: 30-s	1.7	2.1	1.4	2.0	1.4	1.9

radial orbit component, Figure 7(a) shows for day 98 the radial differences between kinematic orbits using SHA and IGS clocks and Precise Scientific Orbits (PSO, sampled at 60 s) from JPL. Figure 7(b) shows the radial differences between kinematic orbits using 30-s clocks of SHA and IGS. The radial differences between the two kinematic orbits shows minor values with mean differences of (0.1, 0.2, –0.2) cm and RMS of (4.8, 3.6, 2.4) cm in the R (radial), T (Along-track), and N (Cross-track) directions, respectively.

Table 4 summarizes the comparisons, showing the mean RMS from days 94–100 of the year 2010. From Table 4 we see that the two orbit sets using 30-s clocks are quite similar, which suggests that our 30-s clocks have the same precision as IGS finals. Clearly, we see that the orbits based on 30-s clocks have much better performance, with the precision of 3-D orbits improved by a factor of up to 2.3.

6 Conclusions

This paper focuses on the 30-s GNSS satellite clocks generation at SHA. We present the efficient and precise epoch-differenced algorithm for the generation of high-rate GNSS satellite clock corrections at SHA. Comparisons show that the densified GPS satellite clocks provided by SHA are closest to the IGR products with a STD of 41 ps and RMS of 82 ps, while GLONASS clocks are closest to GFZ finals with a STD of 85 ps and RMS of 353 ps. These high quality products could contribute well to the IGS combination, especially for the GLONASS products. Applying the densified clocks and conventional 5-min clocks in kinematic PPP and LEO POD, results show that: ① 30-s clocks improve kinematic coordinate accuracy by a factor of up to 2.3; ② kinematic coordinates using the SHA 30-s GNSS clocks have the same accuracy as those using IGS finals and the IGS AC finals; ③ compared to the GPS-only and GLONASS-only kinematic PPP, the combined GPS/GLONASS solution using combined GNSS clocks has the best accuracy, with improvement by up to 34% over the GPS-only solution. The algorithm developed in this paper could be easily implemented as a black-box to current famous scientific GNSS packages and may help to improve

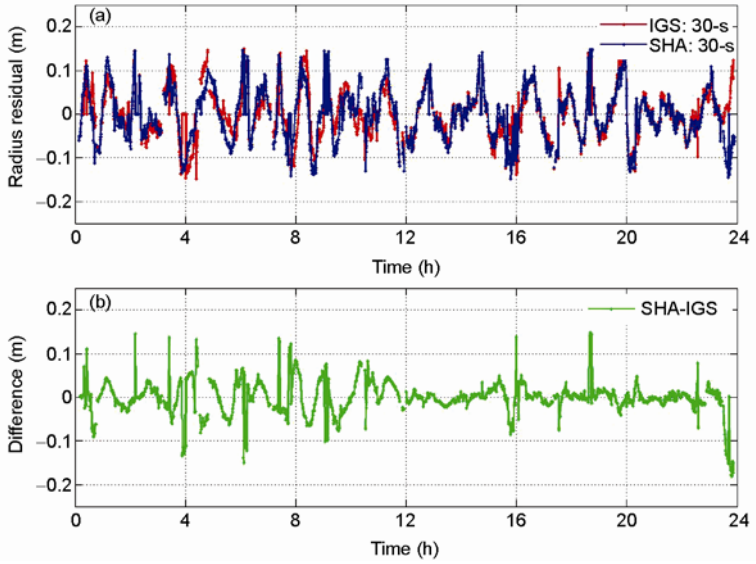

Figure 7 (a) Radial differences between kinematic and JPL PSO orbits when using SHA 30-s clocks or IGS 30-s clocks, GRACE A, day 98 of the year 2010. (b) Radial differences between kinematic orbits when using SHA 30-s clocks and the IGS 30-s clocks.

Table 4 Mean RMS (cm) for differences between kinematic orbits and PSO from JPL, days 94–100, 2010. Kinematic orbits are estimated using precise GPS clocks from IGS final (30-s sampling) and SHA (5-min and 30-s sampling)

	GRACE-A				GRACE-B			
	R	T	N	3-D	R	T	N	3-D
SHA: 5-min	15.9	14.4	14.6	26.0	16.3	15.6	13.4	26.1
SHA: 30-s	6.9	6.4	5.7	11.1	6.7	6.7	6.4	11.6
IGS: 30-s	6.9	6.6	5.5	11.1	7.1	6.1	6.0	11.1

current IGS products. Following the same procedure, we could extend this algorithm for clock densification of 5-s or even higher frequency.

This work was supported by the Program of "One Hundred Talented People" of the Chinese Academy of Sciences, the National Natural Science Foundation of China (Grant Nos. 11273046, 11173049 and 40974018) and the National High Technology Research and Development Program of China (Grant No. 2013AA122402). IGS community is acknowledged for providing Rinex data and orbit and clock products.

1 Zumberge J F, Heflin M B, Jefferson D C, et al. Precise point positioning for the efficient and robust analysis of GPS data from large networks. J Geophys Res, 1997, 102(B3): 5005–5017
2 Bock H. Efficient Methods for Determining Precise Orbits of Low Earth Orbiters Using the Global Positioning System. Dissertation for Doctoral Degree. Berne: Astronomical Institute University of Berne, 2003
3 Svehla D, Rothacher M. Kinematic and reduced-dynamic precise orbit determination of CHAMP satellite over one year using space borne GPS phase zero-differences only. Geophys Res, 2003, 5: 12129
4 Zhu S, Reigber Ch, Koenig R. Integrated adjustment of CHAMP, GRACE, and GPS data. J Geod, 2004, 78: 103–108
5 Banville S, Langley R B. Improving real-time kinematic PPP with instantaneous cycle-slip correction. In: Proceedings of ION GNSS 22nd international technical meeting of the satellite division. Savannah: ION, 2009. 2470–2478
6 Dow J M, Neilan R E, Rizos C. The international GNSS service in a changing landscape of global navigation satellite systems. J Geod, 2009, 83: 191–198
7 Feng Y M, Zheng Y. Efficient interpolations to GPS orbits for precise wide area applications. GPS Solut, 2005, 9: 273–282
8 Wanninger L. Carrier-phase inter-frequency biases of GLONASS receivers. J Geod, 2012, 86: 139–148
9 Chen J P, Wu B, Hu X G, et al. SHA: The GNSS analysis center at SHAO. Lecture Notes Electr Eng, 2012, 160: 213–221
10 Ge M R, Gendt G, Dick G, et al. Improving carrier-phase ambiguity resolution in global GPS network solutions. J Geod, 2005, 79: 103–110
11 Bock H, Dach R, Jaggi A, et al. High-rate GPS clock corrections from CODE: Support of 1 Hz applications. J Geod, 2009, 83: 1083–1094
12 McCarthy D, Petit G. IERS conventions. IERS Technical Note 32, Bundesamt für Kartographie und Geodäsie, Frankfurt am Main, 2003
13 Agrotis L, San P A, Doe J, et al. ESOC's RETINA system and the generation of the IGS RT combination. IGS workshop, 28 June–2 July 2010, Newcastle Upon Tyne, UK
14 Ge M R, Chen J P, Dousa J, et al. A computationally efficient approach for estimating high-rate satellite clock corrections in realtime. GPS Solut, 2012, 16(1): 9–17
15 Allan D. Time and frequency (time-domain) characterization, estimation, and prediction of precision clocks and oscillators. IEEE Trans Ultrason Ferroelectr Freq Contr, 1987, 34(6): 647–654
16 Senior L, Ray R, Beard L. Characterization of periodic variations in the GPS satellite clocks. GPS Solut, 2008, 12: 211–225
17 Senior K, Koppang P, Ray J. Developing an IGS time scale. IEEE Trans Ultrason Ferroelectr Freq Contr, 2003, 50: 585–593
18 Dach R, Hugentobler U, Fridez P, et al. Bernese GPS Software Version 5.0. Bern: Astronomical Institute, University of Bern, 2007
19 Jäggi A, Bock H, Pail R, et al. Highly-reduced dynamic orbits and their use for global gravity field recovery: A simulation study for GOCE. Stud Geophys Geod, 2008, 52(3): 341–359
20 Peng D J, Wu B. Kinematic precise orbit determination for LEO satellites using space-borne dual-frequency GPS measurements (in Chinese). Acta Astron Sin, 2011, 52(6): 495–509